

Synthesis, Characterization, and Receptor Interaction Profiles of Enantiomeric Bile Acids

Bryson W. Katona,[†] Carolyn L. Cummins,[‡] Andrew D. Ferguson,[§] Tingting Li,[‡] Daniel R. Schmidt,[‡] David J. Mangelsdorf,[‡] and Douglas F. Covey^{*†}

Department of Molecular Biology and Pharmacology, Washington University in St. Louis School of Medicine, 660 South Euclid Avenue, St. Louis, Missouri 63110, and Howard Hughes Medical Institute and Department of Pharmacology and Department of Biochemistry, University of Texas Southwestern Medical Center, 6001 Forest Park, Dallas, Texas 75390

Received July 3, 2007

Bile acids are endogenous steroid detergents with receptor-mediated physiologic actions including activation of the G-protein coupled receptor TGR5 and gene regulation mediated by nuclear receptors. In this study, we report the first synthesis of enantiomeric lithocholic acid (*ent*-LCA, **ent-1**) and chenodeoxycholic acid (*ent*-CDCA, **ent-2**) via *ent*-testosterone (**3**). **ent-1** was synthesized in 21 total steps in 4.2% yield, whereas **ent-2** was obtained in 23 total steps in 0.8% yield. Critical micelle concentrations of the enantiomeric bile acids were found to be identical to their natural counterparts. Furthermore, enantiomeric bile acids were also tested for their ability to modulate bile acid activated proteins: farnesoid X receptor, vitamin D receptor, pregnane X receptor, and TGR5. Interestingly, **ent-1** and **ent-2** showed differential interactions with these proteins as compared to their corresponding natural bile acids. These data highlight the potential for using enantioselectivity as a way to distinguish between receptor and nonreceptor-mediated functions of natural bile acids.

Introduction

Bile acids are unique amphipathic steroids that make up the major organic component of secreted bile. The distinct hydrophilic and hydrophobic faces of these steroids are vital for their ability to aid in the digestion and absorption of fats and fat soluble vitamins. In addition to their detergent effects, which are critical for maintaining proper gastrointestinal absorption of nutrients, bile acids have also been shown to be involved in a large variety of other cellular and supracellular processes.

One area of recent interest is the ability of bile acids to interact with numerous members of the nuclear receptor superfamily.¹ This superfamily contains 48 different members in humans, many of which are orphan receptors that have no known ligands. Of these nuclear receptors, bile acids were shown to be the primary endogenous ligands of FXR.^{2–4} Activation of this receptor by bile acids prevents the accumulation of toxic concentrations of these steroids in cells by decreasing their synthesis and import, increasing their excretion from cells, and inducing the expression of proteins that sequester them.⁵

Bile acids have also been shown to function as ligands for PXR as well as VDR.^{6–8} Like FXR, the binding of bile acids to these receptors results in the metabolism of these steroids, thus preventing the toxic accumulation of these detergents inside cells. However, unlike FXR, bile acids are not the only known endogenous ligands of these two receptors: PXR can be activated by (*5β*)-pregnane-3,20-dione, which is a progesterone reduction product, as well as a large and diverse class of

xenobiotics and drugs,⁹ and VDR can be activated by 1,25-(OH)₂-vitamin D₃.¹

Modulation of FXR, PXR, and VDR by specific agonists and antagonists could have important therapeutic applications. For instance, it was shown that the potent FXR agonist 3-[2-[2-chloro-4-[[3-(2,6-dichlorophenyl)-5-(1-methylethyl)-4-isoxazolyl]-methoxy]phenyl]ethenyl]benzoic acid (GW4064, **4**) could be used to prevent liver damage caused by cholestatic disease and prevent cholesterol gallstone disease.¹⁰ Agonist **4** is thought to accomplish these protective effects by promoting bile acid and phospholipid excretion and repressing bile acid synthesis. On the other hand, FXR antagonists may be useful therapeutically to increase the conversion of cholesterol to bile acids resulting in lower LDL levels in hyperlipidemic patients. The plant sterol and FXR antagonist guggulsterone (pregna-4,17(20)-diene-3,16-dione) was recently tested for this indication but failed to show any improvement in LDL cholesterol levels.¹¹ It was later discovered that guggulsterone lacks specificity and is also a potent activator of PXR.¹² Therefore, there is still a promising future ahead for the development of drugs to modulate FXR activity if increased selectivity is achieved. Compounds acting as agonists toward PXR have also been investigated as treatments for various pathologic conditions.¹³ Specifically, the PXR agonist rifampicin, in addition to having anti-microbial properties, has been shown to alleviate cholestasis and pruritis resulting from cholestatic disease.⁹ Furthermore, ligands for VDR have also been investigated. The interest in these ligands has centered around their potential anti-inflammatory, anti-cancer, and anti-microbial properties.^{14,15}

The endocrine properties of bile acids have long been thought to be mainly due to their actions in the enterohepatic system. Recent evidence suggests that bile acids may also act in the periphery through activation of TGR5, a GPCR that is activated by selected bile acids [including CDCA (**2**) and LCA (**1**)].^{16,17} Wantanabe and colleagues¹⁸ have recently found that bile acids can increase whole body energy expenditure by promoting intracellular thyroid hormone activation in brown adipose tissue.

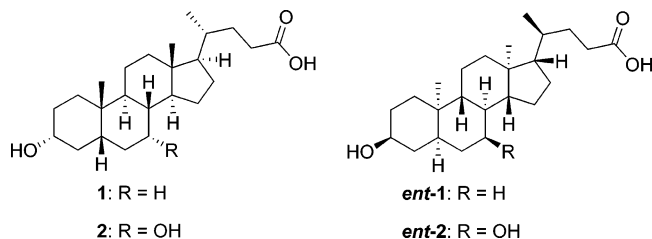
* Corresponding author. Tel.: (314) 362-1726; fax: (314) 362-7058; e-mail: dcovey@wustl.edu.

[†] Washington University in St. Louis School of Medicine.

[‡] Howard Hughes Medical Institute and Department of Pharmacology, University of Texas Southwestern Medical Center.

[§] Department of Biochemistry, University of Texas Southwestern Medical Center.

^a Abbreviations: LCA, lithocholic acid; CDCA, chenodeoxycholic acid; GPCR, G-protein coupled receptor; FXR, farnesoid X receptor; VDR, vitamin D receptor; PXR, pregnane X receptor; cmc, critical micelle concentration; SRC1, steroid receptor coactivator 1; RXR, retinoid X receptor; BSEP, bile salt export pump; SHP, small heterodimer partner; IBABP, ileal bile acid binding protein.

Chart 1. Natural and Enantiomeric Lithocholic Acid (**1** and *ent-1*) and Chenodeoxycholic Acid (**2** and *ent-2*)

An important unanswered question in the field of bile acid biology concerns the inability to dissect the relative contribution of the detergent properties of natural bile acids from their receptor-mediated properties. While efforts have focused on generating high affinity synthetic ligands to selectively activate the receptors, one class of derivatives that has not yet been examined is bile acid enantiomers. Enantiomeric compounds are non-superimposable mirror images of one another. Complementary pairs of enantiomers have identical physical properties with the exception of their optical rotations, which are equal in magnitude and opposite in direction. However, despite their identical physical properties (other than optical rotation), enantiomers have different three-dimensional structures that result from their opposite stereochemical configurations at each asymmetric carbon. Presumably, this could allow different enantiomers to uniquely interact with proteins because of their spatially distinct three-dimensional ligand binding pockets.

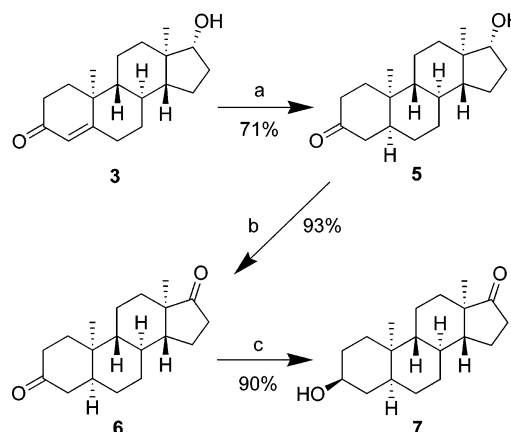
In this study, we report the first syntheses of the enantiomers of the secondary bile acid **1** (*ent*-LCA, *ent-1*) and the primary bile acid **2** (*ent*-CDCA, *ent-2*) (Chart 1). We determined that these bile acid enantiomers have identical cmcs as compared to their natural counterparts. These compounds were then tested to determine their abilities to interact with the bile acid sensing nuclear receptors FXR, PXR, and VDR and the newly orphanized GPCR, TGR5.^{16,17}

Results

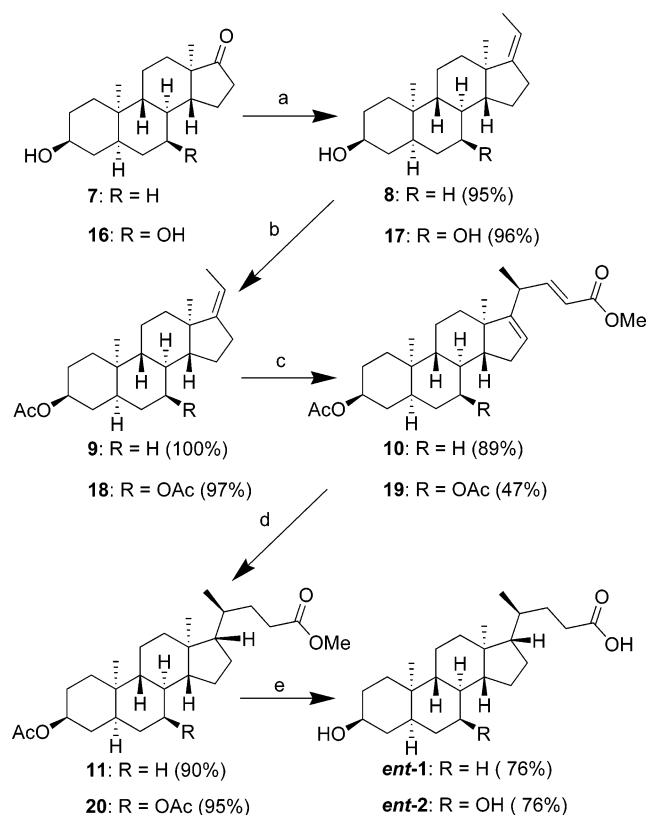
Chemistry. Both *ent-1* and *ent-2* were prepared from an *ent*-testosterone (**3**) precursor. This unnatural *ent*-steroid **3** was prepared from achiral 2-methyl-1,3-cyclopentanone according to previously published precedents in 13 steps with a 12.1% yield.^{19,20}

The synthesis of *ent-1* started with the conversion of *ent*-steroid **3** to *ent*-etiocolanolone (**7**) as described by us previously.²¹ Briefly, hydrogenation of **3** under basic conditions gave the *cis*-fused saturated *ent*-steroid **5** (Scheme 1).²² Jones oxidation led to the dione **6**, and then selective reduction of the 3-ketone under low temperature conditions with lithium tri-*t*-butoxyaluminumhydride gave **7** in high yield.²³

The side chain was constructed in a manner similar to that used for the construction of the *ent*-desmosterol side chain (Scheme 2).²⁴ A Wittig reaction was first performed to add the 20- and 21-carbons to *ent*-steroid **7** to give primarily the *Z* isomer **8**. Before the rest of the side chain could be added, the 3-hydroxyl group had to be protected as an acetate. This was done with the use of 4-dimethylaminopyridine (DMAP) as a catalyst to give the protected olefin **9**. The remainder of the side chain was added through an ene reaction with methyl propiolate, catalyzed by diethylaluminum chloride. This gave the diene **10**, which was hydrogenated with a palladium catalyst to give the saturated ester **11**. Finally, the acetate protecting group on the 3-hydroxyl was removed, and the side chain methyl ester was hydrolyzed under basic conditions to yield *ent-1*.²⁵

Scheme 1^a

^a Reagents (a) Pd/C, H₂ (45 psi), KOH, *i*-PrOH, 18 h; (b) Jones reagent, acetone, 30 min; and (c) Li(*t*-BuO)₃AlH, THF, -42 °C, 4 h.

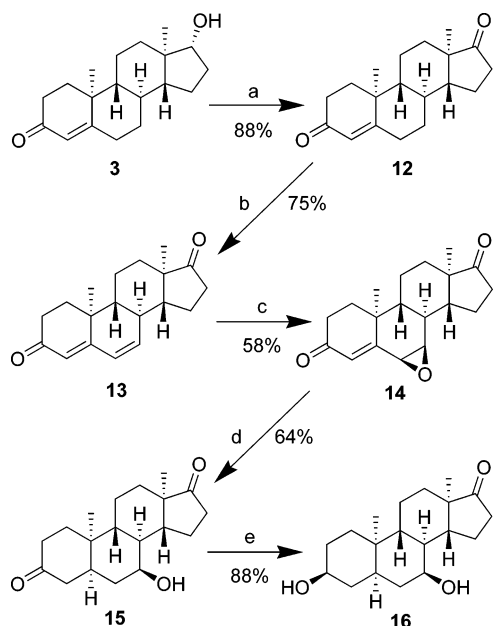
Scheme 2^a

^a Reagents: (a) EtPPh₃Br, *t*-BuOK, THF, reflux, 2 h; (b) Ac₂O, DMAP, pyridine; (c) methyl propiolate, Et₂AlCl, toluene; (d) Pd/C, H₂ (60 psi), MeOH; and (e) KOH, EtOH, reflux, 18 h.

Ultimately, *ent-1* was obtained in 8 steps from **3** in a 34.4% yield and in 21 total steps with a 4.2% yield from 2-methyl-1,3-cyclopentanone.

Both **1** and *ent-1* were white solids, with identical melting points, IR spectra, ¹H and ¹³C NMR spectra, and hydrogen and carbon elemental analyses. The only physical characteristic that differed between the two compounds was their optical rotations, which were of equal magnitude and opposite direction.

The synthesis of *ent-2* was performed using a slightly different route because a 7-hydroxyl group had to be added to the molecule. Starting from *ent*-steroid **3**, the 17-hydroxyl group was first oxidized by using Jones reagent to give *ent*-androstenedione (**12**, Scheme 3). Next, enone **12** was converted to

Scheme 3^a

^a Reagents: (a) Jones reagent, acetone, 30 min; (b) *p*-chloranil, AcOH, toluene, reflux, 1 h; (c) *m*-CPBA, CH₂Cl₂, 4 °C, 2 days; (d) Pd/C, H₂ (30 psi), pyridine, 18 h; and (e) Li(*t*-BuO)₃AlH, THF, -42 °C, 4 h.

dienone **13** through a dehydrogenation reaction using *p*-chloranil in acetic acid.²⁶ This was a time sensitive reaction, with reflux times over 1 h producing an increased amount of side products. The Δ⁶ double bond was then selectively epoxidized on the less sterically hindered face opposite the 18- and 19-methyl groups by using *m*CPBA at low temperatures to give epoxyenone **14**.²⁶ Hydrogenation over palladium in pyridine with low H₂ pressures gave dione **15**.²⁶ This hydrogenation had two important roles: opening the 6,7-epoxide to give the 7-hydroxyl group, and setting the cis-ring fusion at the A,B ring junction. Finally, the 3-ketone of *ent*-steroid **15** was selectively reduced at low temperatures to give dihydroxy compound **16**.²⁶

The addition of the bile acid side chain to *ent*-steroid **16** was carried out in the same way as for *ent*-**1** (Scheme 2). A Wittig reaction was used to add two carbons to **16**, giving the olefin **17**.²⁷ The presence of the 7-hydroxyl group in *ent*-steroid **16** did not interfere with the *Z* orientation of the major product. Esterification of both the 3- and the 7-hydroxyl groups with acetic anhydride was successful to yield diacetate **18**; however, a longer reaction time had to be employed due to the decreased reactivity of the 7-hydroxyl group. Addition of the rest of the side chain via an ene reaction yielded **19**. This reaction would not proceed to completion; however, most of the unreacted starting material was recovered during purification. Saturation of both double bonds gave *ent*-steroid **20**, and then hydrolysis of both acetate protecting groups and the side chain methyl ester yielded *ent*-**2**. This compound was synthesized in 10 steps with an overall yield of 6.7% from **3**, and from 2-methyl-1,3-cyclopentanedione it was synthesized in 23 steps with a 0.8% yield. Furthermore, like **1** and *ent*-**1**, **2** and *ent*-**2** had identical physical properties except for their optical rotations, which were of equal magnitude and opposite direction.

cmc Determination. The cmcs of the natural and enantiomeric steroids were evaluated by a previously validated dye solubilization method used for measuring the cmc of the sodium salt of **2**.²⁸ The dye solubilization method utilizes an achiral, water insoluble dye, Orange OT, which can be solubilized by bile acid micelles. In these experiments, the sodium salt of each

bile acid was used due to the increased aqueous solubility of the salt as compared to the acid.

Representative plots of absorbance as a function of concentration looked similar for the salts of **1** (Figure 1A) and *ent*-**1** (Figure 1B). When these absorbance plots were used to calculate the cmcs, it was found that **1** had a cmc of 278.6 ± 7.3 μM, whereas *ent*-**1** had a cmc of 273.9 ± 7.0 μM, which was not significantly different from **1** (Table 1). This is the first report of using this dye solubilization method to determine the cmc for **1**; therefore, there are no cmc values using this method to compare to the one obtained. However, previous reports using different methods have estimated the cmc of **1** to be around 200 μM.²⁹

Representative absorbance plots were also similar for the salts of **2** (Figure 1C) and *ent*-**2** (Figure 1D). cmcs calculated from these plots gave 10.08 ± 0.89 mM for **2** and 10.42 ± 0.30 mM for *ent*-**2** (Table 1). These two values were not significantly different and were in close agreement with the previously reported cmc value of 10 mM for **2** determined by this method.²⁸

Nuclear Receptor Biology. The abilities of *ent*-**1** and *ent*-**2** to activate several bile acid responsive human nuclear receptors (FXR, VDR, and PXR) were examined and compared to their natural counterparts **1** and **2**. To screen for nuclear receptor activation, fusion proteins containing the ligand binding domain of the nuclear receptor fused to the DNA binding domain of GAL4 were tested with a luciferase reporter specific for the GAL4 DNA binding domain. Natural and enantiomeric bile acids were examined at concentrations of 5, 20, and 50 μM. As a negative control, the GAL4-DNA binding domain alone was tested, and no significant activation was observed with all bile acid ligands (**1**, *ent*-**1**, **2**, and *ent*-**2**; data not shown).

In the GAL4-hFXR agonist studies, **2** and *ent*-**2** showed marked differences in their ability to induce activation. Compound **2**, the strongest physiologic bile acid activator of FXR, showed increasing activation of GAL4-hFXR in a dose dependent manner, with 27-fold higher activation at 50 μM as compared to control.²⁻⁴ In contrast, *ent*-**2** showed no significant activation of GAL4-hFXR at any of the concentrations tested (Figure 2A). Compounds **1** and *ent*-**1** both showed modest activation of GAL4-hFXR in a concentration dependent manner with a 2–3-fold activation over control at the highest concentration (50 μM, Figure 2A). The difference in activation of GAL4-hFXR by **2** and **1** was consistent with that observed in previous literature reports.³

For VDR, the most potent natural non-secosteroid ligand is **1**, and activation of GAL4-hVDR by this bile acid resulted in a 26-fold increase in luciferase activity at 50 μM as compared to control (Figure 2A).⁸ However, even at 50 μM, *ent*-**1** showed no significant activation of this nuclear receptor. Furthermore, neither **2** nor *ent*-**2** showed any significant activation toward GAL4-hVDR.

Finally, activation of GAL4-hPXR was analyzed for these natural and enantiomeric bile acids. PXR is a xenobiotic receptor that is considered to be the most promiscuous receptor in the superfamily because of the wide variety of ligands that it can accommodate.³⁰ All four bile acids tested (**2**, *ent*-**2**, **1**, and *ent*-**1**) showed significant activation of GAL4-hPXR at 20 and 50 μM (Figure 2A), with *ent*-**2** showing the most significant activation (6-fold).

The natural and enantiomeric bile acids were analyzed also for their ability to antagonize GAL4-hFXR activation by 1 μM synthetic FXR agonist **4**.^{31,32} Compounds **2** and *ent*-**2** showed similar profiles, each showing only minimal antagonism of

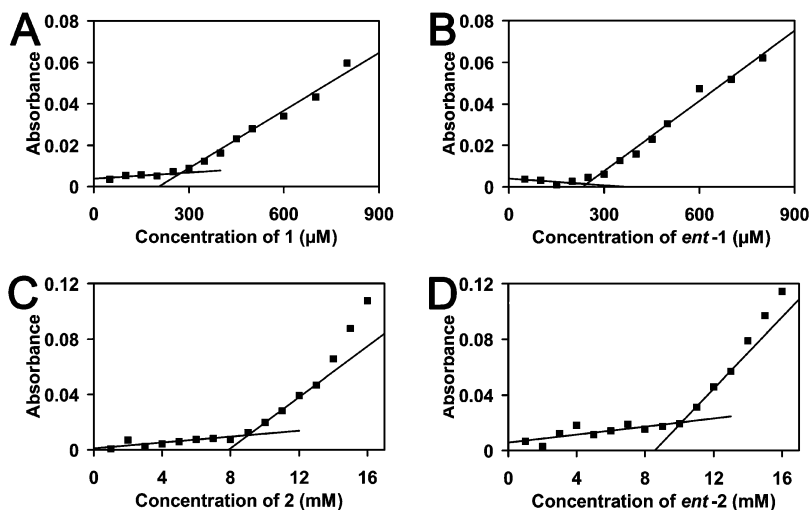


Figure 1. cmc determination of natural and enantiomeric bile acids. Representative absorbance vs bile salt concentration plots used for the determination of the cmc by the Orange OT dye solubilization method. Absorbance readings were taken at 483 nm, and linear best-fit lines are drawn according to the experimental methods. (A) **1**, (B) *ent-1*, (C) **2**, and (D) *ent-2*.

Table 1. cmc Values Determined from the Orange OT Dye Solubilization Method^a

	cmc	SD
1	278.6 μM	7.3 μM
<i>ent-1</i>	273.9 μM ^b	7.0 μM
2	10.08 mM	0.89 mM
<i>ent-2</i>	10.42 mM ^c	0.30 mM

^a cmc reported is the average of three independent experiments using a different aqueous bile salt standard for each experiment. Error bars represent SD calculated with $N = 3$. ^b $p > 0.4$, as compared to the value calculated for **1**. ^c $p > 0.5$, as compared to the value calculated for **2**.

GAL4-hFXR activation (Figure 2B). Even at 100 μM , neither **2** nor *ent-2* was able to antagonize by 50% the activation of GAL4-hFXR by agonist **4**. Compounds **1** and *ent-1* proved to be more effective at antagonizing the activation of GAL4-hFXR by **4**. This is likely because **1** and *ent-1* are acting as partial agonists thereby competing for ligand binding.

An important property of ligand activated nuclear receptors is their ability to recruit coactivator proteins, which then allows active gene transcription to occur. A GAL4-fusion protein of the steroid receptor coactivator 1 (SRC1) interaction domain 2 was tested in combination with VP16-hFXR, a constitutively activated form of the receptor.² A strong interaction was observed in the presence of FXR agonist **4** (data not shown) and natural steroid **2** (Figure 2C). In contrast, no activation was observed with *ent-2*, whereas small but equivalent activation was seen with **1** and *ent-1* (Figure 2C). The ability of *ent-1* to cause a positive interaction between these proteins suggests that this *ent*-bile acid is truly binding to the ligand pocket and causing a conformational change required to recruit a coactivator.

We also tested full-length human FXR (hFXR) for activation by *ent*-bile acids on an FXR response element consisting of a multimerized IR-1 repeat derived from the mIBABP promoter upstream of a luciferase reporter. The ability of RXR α to enhance the response to bile acid treatment by heterodimerizing with FXR was also examined. Both **1** and *ent-1* showed equivalent activation of full length FXR at 50 μM (Figure 2D). In contrast, **2** strongly activated (16.8-fold) the FXR/RXR heterodimer, whereas no significant activation was seen with *ent-2*.

To assess how the natural and enantiomeric bile acids could regulate gene transcription, RT-PCR was performed on FXR responsive genes in the human liver cell lines Huh7 and HepG2

and the human colon carcinoma cell line Caco-2. Strong activation of the bile salt export pump (BSEP) and the small heterodimer partner (SHP) was seen in Huh7 cells treated with FXR agonist **4** (Figure 3A). Compounds **2**, **1**, and *ent-1* also significantly activated these positively regulated FXR target genes, in agreement with the GAL4-hFXR reporter assay (Figure 3A). Cytochrome P450 7A1 (CYP7A1) is the rate-limiting enzyme in the conversion of cholesterol to primary bile acids. Negative regulation of CYP7A1 by bile acids accounts for the feedback inhibition of bile acid synthesis and is critical for protecting the liver from the buildup of toxic bile acids. The mRNA of CYP7A1 was not detectable in Huh7 cells. Therefore, further experiments were performed in HepG2 cells. HepG2 cells were treated with **2** and *ent-2* at a concentration of 25 μM , while a concentration of 10 μM was used for **1** and *ent-1* due to the increased toxicity of these molecules in this cell line. BSEP mRNA was significantly increased when HepG2 cells were treated with FXR agonist **4** as well as steroid **2** (Figure 3B). No significant activation was noted for *ent-2* or for **1** and *ent-1* at the lower concentration. SHP expression was significantly increased by **2** and *ent-1*, whereas all natural and *ent*-bile acids significantly decreased CYP7A1 expression (Figure 3B). While SHP is known to be involved in the negative regulation of CYP7A1, these data suggest that a SHP independent mechanism of CYP7A1 repression by bile acids is also active in this cell line.

The intestine is another critical site for FXR activation as high levels of bile acids circulate in this organ. The colon carcinoma cell line Caco-2 differentiates into small intestine-like cells when grown for 3 weeks post-confluence. The FXR target gene ileal bile acid binding protein (IBABP) was strongly induced by FXR agonist **4** and **2** in this cell line after 6 days of treatment (Figure 3C). In contrast, no activation by *ent-2*, **1**, or *ent-1* was observed under these conditions.

Molecular Modeling. In an attempt to rationalize the activation profiles of the natural and enantiomeric bile acids (**2**, *ent-2*, **1**, and *ent-1*), these compounds were modeled into the ligand binding pocket of FXR. Using the X-ray crystallographic structure of FXR in complex with 6-ethyl CDCA (6ECDCA) as the structural template, these bile acids were superimposed onto the 6ECDCA molecule by maintaining the relative orientations of the 3 α -hydroxyl on the A ring and the methyl groups at positions 18 and 19.³³

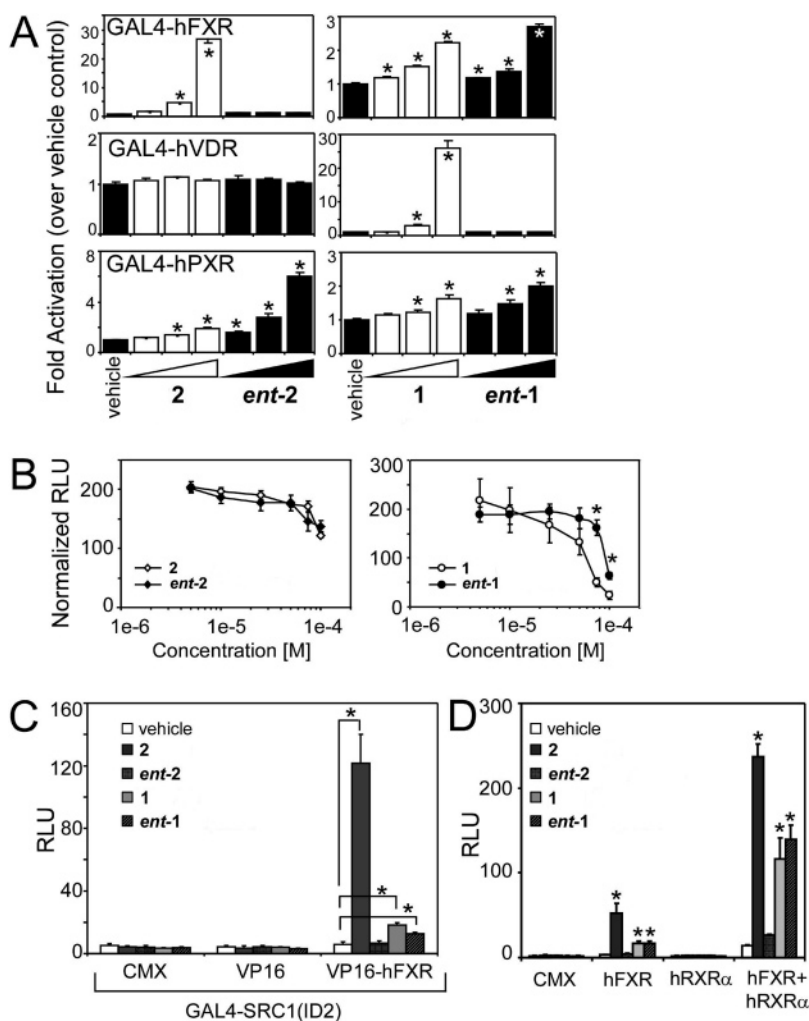


Figure 2. Selective nuclear receptor activation by natural and enantiomeric bile acids in HEK293 cells. (A) Fold activation of GAL4-hFXR, GAL4-hVDR, or GAL4-hPXR by **2**, *ent-2*, **1**, and *ent-1* at 5, 20, and 50 μM . Activation was normalized to vehicle control (EtOH). (B) Antagonist activity of **2** and *ent-2* or **1** and *ent-1* on GAL4-hFXR in HEK293 cells activated using a synthetic FXR agonist **4** (1 μM). Values were normalized to vehicle control (EtOH) at each concentration. (C) Ligand dependent interaction of VP16-hFXR with the coactivator SRC-1 (interaction domain 2, ID2) measured by mammalian two-hybrid analysis using GAL4-SRC-1(ID2), FXR agonist **4** (1 μM) and bile acids (50 μM). Empty CMX and CMX-VP16 were used as negative controls. (D) Ligand dependent activation of full-length hFXR and hRXR α by bile acids (50 μM) measured using the FXRE₃₃ TK-Luc reporter derived from the IR-1 of mouse IBABP. RLU, relative light units. For all experiments $N = 3$, mean \pm SD, * $p < 0.05$.

Given the minor chemical difference between **2** and 6ECDCA, the predicted orientation of **2** in the ligand binding site of FXR is most likely identical to that observed in the FXR–6ECDCA complex (Figure 4A).³³ With the exception of residues I359 and F363 from helix 7, all interactions between FXR and **2** should also be conserved. When *ent-2* is modeled in the ligand binding pocket, its 3 α -hydroxyl could potentially form hydrogen bonds with residue H444 from helix 10/11 and residue Y358 from helix 7 and van der Waals interactions with residues F326 from helix 5 (Figure 4A). It has been previously shown that the relative affinities of various bile acids are strongly influenced by the presence of α -hydroxyl groups at the 7-position on ring B and at the 12-position on ring C.³³ In our model, the 7 α -hydroxyl of *ent-2* would be positioned on the opposite side of the ligand binding pocket (as compared to **2** and 6ECDCA) and would be unable to form a hydrogen bond with residue Y366 from helix 7. Moreover, this hydrophobic region of the ligand binding pocket of FXR lacks suitable hydrogen bond donors/acceptors to accommodate the 7 α -hydroxyl group of *ent-2*. Hence, according to this proposed model, the binding of *ent-2* would be energetically unfavorable and unlikely to activate FXR even at high concentrations.

The bile acids **1** and *ent-1* were also modeled in the ligand binding pocket of FXR (Figure 4B). Electrostatic and van der Waals interactions between 3 α -hydroxyl and residue F326 from helix 5, residue Y358 from helix 7, and residue H444 from helix 10/11 would be maintained. Given that **1** and *ent-1* both lack a 7 α -hydroxyl, residue Y366 from helix 7 would not interact with the B ring of either enantiomer, and the relative binding affinity of **1** and *ent-1*, and the associated activation of FXR, would be substantially reduced in comparison to **2** and 6ECDCA.

Interaction with TGR5. Recent evidence has suggested that bile acids may exert their physiologic effects partially outside of the enterohepatic system through the activation of the GPCR TGR5.^{16–18,34} To test whether the natural and *ent*-bile acids had any selectivity for this receptor, we developed a reporter assay in which HEK293 cells were cotransfected with TGR5 (Figure 5) or control vector (data not shown) and treated with bile acids. A positive interaction with TGR5 was detected by measuring the elevation of intracellular cAMP. The synthetic TGR5 agonist benzyl 2-keto-6-methyl-4-(2-thienyl)-1,2,3,4-tetrahydropyrimidine-5-carboxylate (**21**) and forskolin (**22**), which is an activator of adenylate cyclase, gave 7.5- and 16.5-fold increases in cAMP

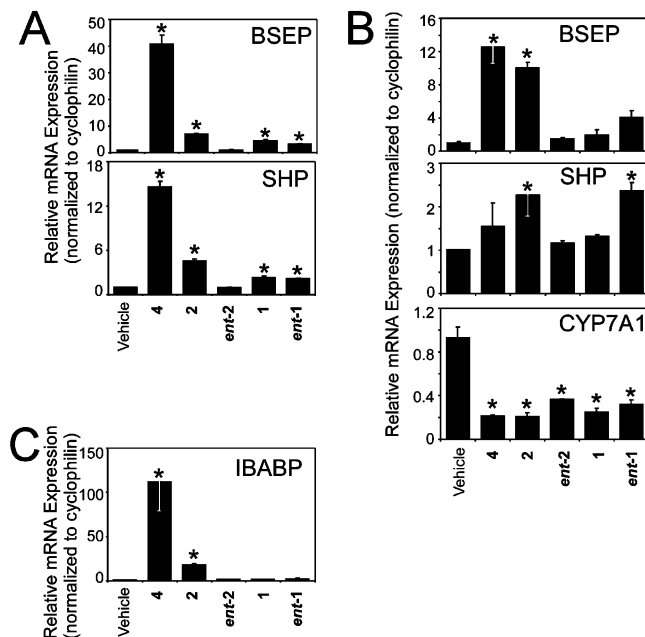


Figure 3. Activation of FXR responsive genes in Huh7, HepG2, and Caco-2 cells by natural and enantiomeric bile acids. (A) Huh7 cells were treated with 1 μ M FXR agonist **4** and 20 μ M bile acids for 18 h before harvesting RNA. (B) HepG2 cells were treated with 1 μ M FXR agonist **4** and 25 μ M **2** and *ent-2* or 10 μ M **1** and *ent-1* for 18 h before harvesting RNA. (C) Caco-2 cells were grown for 23 days post-confluence and then treated with 1 μ M FXR agonist **4** or 25 μ M bile acids for 6 days. Gene expression was measured by real-time QPCR, normalized against the housekeeping gene cyclophilin, and plotted relative to vehicle control. Data represent the mean \pm SD ($N = 3$, except C, where $N = 2$). *Significantly different from vehicle control ($p < 0.05$).

levels, respectively, over vehicle control. In contrast, only **2** and **1** significantly increased cAMP levels (and not *ent-2* and *ent-1*), demonstrating the specificity of this receptor for the natural bile acids.

Discussion

The enantiomers of many biologically relevant steroids have been synthesized and used to investigate a wide variety of biological problems.³⁵ One area of enantiomeric steroid chemistry that remains poorly explored, both chemically and biologically, is A,B cis-fused steroids, of which the bile acids are the most notable members. Although many reactions have been performed on natural A,B cis-fused steroids, few of these reactions have ever been applied to enantiomeric systems. Therefore, to our knowledge, our synthesis of *ent-1* and *ent-2* from an *ent*-steroid backbone **3** is the first reported synthesis of these enantiomeric bile acids. The synthesis of *ent*-bile acids from **3** involves many steps and proves to be a long synthetic route; however, there are currently no better methods for assembling the steroid ring system with the bile acid side chain in the unnatural configuration. Of the two *ent*-bile acids synthesized, the synthesis of *ent-2* is more lengthy and provides a lower yield than *ent-1*, due to the difficulty of installing the 7-hydroxyl group in this more hydrophilic primary bile acid.

Physical characterization of the *ent*-bile acids showed that besides optical rotation, the *ent*-bile acids were physically equivalent to the natural bile acids. This result was expected because by definition the enantiomers should be completely identical in all physical properties except optical rotation. Special interest was given to the ability of the natural and enantiomeric bile acids to aggregate as micelles in a similar fashion. To

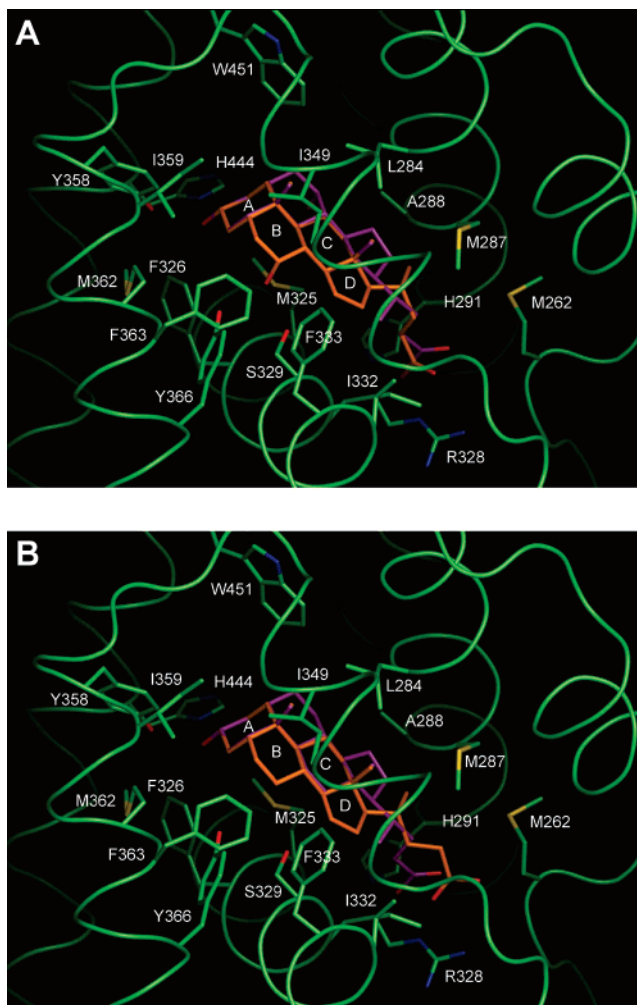


Figure 4. Model of natural and enantiomeric bile acids in the FXR ligand binding pocket. (A) Superposition of **2** (orange) and *ent-2* (purple) on the 6ECDCA/FXR crystal structure maintaining the position of the 3 α -hydroxyl group and the 18 and 19 methyl groups. The steroid ring system of **2** as well as select amino acids within the ligand binding pocket are labeled. (B) Superposition of **1** (orange) and *ent-1* (purple) on the 6ECDCA/FXR crystal structure using the same criteria as above.

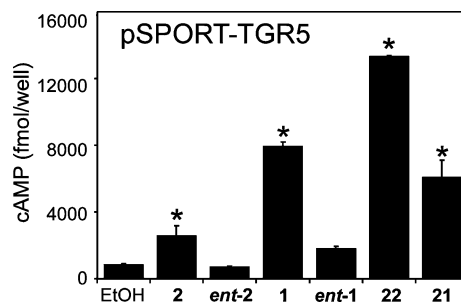


Figure 5. Selective activation of the G-protein coupled receptor TGR5 by natural bile acids. HEK293 cells were transfected with TGR5 and assayed for TGR5 activation by monitoring the production of cAMP. The synthetic TGR5 agonist **21** (10 μ M) and forskolin (**22**, 100 μ M) were used as positive controls. Natural and *ent*-bile acids were dosed at 10 μ M. Data represent the mean \pm SD ($N = 2$). *Significantly different from vehicle control ($p < 0.05$).

address this issue, the cmcs were determined for the *ent*-bile acids, and these were shown to be identical to the natural compounds. Although the cmc is a measure of detergent activity, an achiral molecule was used to determine this value. By contrast, cell membrane lipids are chiral molecules, and having identical cmcs does not necessarily mean that the natural and

enantiomeric bile acids will solubilize cell membrane lipids in the same way. Thus far, in spite of the fact that the head groups of cellular membrane lipids contain one or more chiral centers, biophysical studies of cholesterol enantiomers and anesthetic steroid enantiomers with model membrane lipids have failed to detect enantioselectivity for steroid–membrane lipid interactions.^{36,37} Hence, it also seems possible that the natural and enantiomeric bile acids would behave similarly when solubilizing cellular membrane lipids as well. Studies with the *ent*-bile acids and model membrane lipids are planned to address this question.

The interactions of natural and enantiomeric bile acids with nuclear receptors and TGR5 were found to be enantioselective, with the natural and enantiomeric bile acids showing different interaction profiles. This is the expected result when considering that these proteins have a defined architecture and are themselves chiral molecules. Therefore, when chiral proteins interact with chiral molecules such as bile acids, the spatial orientation of the molecules becomes important for determining the extent of the interaction. Thus, it is expected that enantiomers with different chiralities at each chiral carbon should interact differently with chiral proteins.

One major trend can be appreciated when examining the nuclear receptor and TGR5 activation data. Whenever a bile acid caused strong activation of a receptor, its enantiomer did not. This is true for **2**, which strongly activated GAL4-hFXR, while its enantiomer *ent*-**2** showed no appreciable activation. Also, **1** strongly activated GAL4-hVDR, and *ent*-**1** showed no activation of this nuclear receptor. Similarly, **2** and **1** activated TGR5, whereas the enantiomers did not. However, it is interesting to note that the natural bile acids were not the only molecules that were capable of activating the nuclear receptors. *ent*-**2** proved to be a more effective activator of GAL4-hFXR as compared to **2**. Whereas PXR is a notoriously promiscuous receptor with a very large ligand binding pocket,³⁰ it was a surprise to discover that **1** and *ent*-**1** equally activated GAL4-hFXR. The specific interaction of *ent*-**1** with FXR was confirmed using a two-hybrid coactivator recruitment assay in which the coactivator was found to be associated with the receptor in the presence of *ent*-**1**. Furthermore, *ent*-**1** was shown to be as effective as **1** at activating full-length hFXR on an FXR responsive reporter.

An attempt was made to rationalize the differences seen with GAL4-hFXR through the use of molecular modeling. Bile acids themselves have distinct convex hydrophobic and concave hydrophilic faces that are specifically tailored to complement the physicochemical properties of the ligand binding site of FXR. For example, **2** shows strong GAL4-hFXR activation, and superimposition of this ligand on 6ECDCA supported this observation by showing how both 3 α - and 7 α -hydroxyl groups of **2** can interact with other hydrogen bond donors/acceptors of FXR. However, *ent*-**2** does not activate FXR, and when aligned in the same fashion in this model, the 7 α -hydroxyl has no hydrogen bond acceptor/donor to interact with and is in a relatively hydrophobic region of the binding pocket. This makes the binding of this ligand unfavorable and can possibly explain its poor ability to activate GAL4-hFXR. In the case of **1** and *ent*-**1**, both of these bile acids lack a 7 α -hydroxyl group; therefore, they can both only hydrogen bond with their 3 α -hydroxyl. Although **1** and *ent*-**1** have only one hydroxyl group participating in hydrogen bonding, they may activate GAL4-hFXR better than *ent*-**2** because they do not have another hydroxyl group in an unfavorable hydrophobic region of the protein. From the models that were generated, it appears that

the ligand binding pocket of FXR is large enough to accommodate each of the natural and enantiomeric bile acids tested, which could explain the ability of natural and enantiomeric bile acids to compete with the activation of GAL4-hFXR by the synthetic FXR agonist **4**.

To assess whether activation of the nuclear receptors by the natural and *ent*-bile acids extends to a native cellular context, we examined the gene expression of FXR target genes in selected cell lines after treatment with bile acids. The expression of BSEP and SHP in the Huh7 cell line showed a perfect correlation with the GAL4–nuclear receptor interaction data. These target genes are both directly regulated by FXR. In contrast, the expression of CYP7A1, a negatively regulated FXR target gene, in HepG2 cells was significantly repressed by all bile acids tested, demonstrating additional non-FXR-mediated pathways present in this cell line. The repression of CYP7A1 by *ent*-**2** may occur via PXR since this receptor has also been implicated in the regulation of CYP7A1¹² or could also occur through a non-nuclear receptor-mediated mechanism.

Taken together, these results illustrate that the *ent*-bile acids have very different biological activation profiles as compared to their natural counterparts and provide interesting probes to examine the effects of activating/antagonizing different combinations of receptors. Furthermore, the *ent*-bile acids reported herein provide the much needed tools to dissect the relative contribution of the detergent properties of bile acids from their protein-mediated interactions.

Conclusion

This work has shown that *ent*-bile acids can be synthesized, have expected identical physical properties including cmcs, and show a differential ability to interact with signaling proteins such as nuclear receptors and TGR5. Besides being interesting selective nuclear receptor modulators themselves, *ent*-bile acids could also be used to probe the nonreceptor-mediated functions of the natural steroids. Biophysical studies using steroid enantiomers with natural membrane lipids have not shown enantioselective interactions.^{36,37} Thus, if *ent*-bile acids act as identical detergents of cellular lipids, these molecules could be utilized to unravel which bile acid effects are due to detergent versus receptor-mediated interactions. In conclusion, these compounds show great promise to provide a novel method to address some of the important questions pertaining to bile acid biology that have remained unanswered to date.

Experimental Procedures

Chemistry. Melting points were determined on a Kofler microhot stage and are uncorrected. IR spectra were recorded as films on a NaCl plate or as KBr disks with a PerkinElmer 1710 FT-IR Spectrum One spectrophotometer. Solvents were used either as purchased or they were dried and purified by standard methodology. Flash chromatography was performed using silica gel (32–63 μ m) purchased from Scientific Adsorbents. Optical rotations were determined on a PerkinElmer Model 341 polarimeter. NMR spectra were taken in CDCl₃ or CD₃OD with a 5 mm probe on a Varian Gemini 2000 that operates at 300 MHz (¹H) and 75 MHz (¹³C). ¹H spectra in CDCl₃ were referenced to δ 7.26, while those in CD₃OD were referenced to δ 4.87. ¹³C spectra in CDCl₃ were referenced to δ 77.00, while those in CD₃OD were referenced to δ 49.15. Elemental analyses were performed by M-H-W Laboratories.

ent-Lithocholic Acid (*ent*-**1**). *ent*-Steroid **11** (1.04 g, 2.4 mmol) was dissolved in ethanol (50 mL) and refluxed with 20% aqueous KOH (50 mL) for 18 h. After cooling to room temperature, the solution was acidified with 6 N HCl until a precipitate was formed. The resulting suspension was then extracted with CH₂Cl₂ (150 mL \times 3). The organic extracts were combined, and the solvent was

removed in vacuo to yield a yellow solid. Column chromatography (silica gel, 50% EtOAc/49% hexanes/1% AcOH) of the product gave a white solid that was recrystallized from MeOH to yield **ent-1** (0.69 g, 76%) as a white solid: mp 185–187 °C (1 lit³⁸ mp 184–186 °C); $[\alpha]_D^{25} = -37.1$ ($c = 0.4$, EtOH) (1 lit³⁸ $[\alpha]_D^{20} = +33.7$ ($c = 1.5$, EtOH)); IR 3428, 1707 cm⁻¹; ¹H NMR (CD₃OD) δ 3.53–3.48 (m, 1H), 0.93 (d, 3H, $J = 6.3$ Hz), 0.92 (s, 3H), 0.67 (s, 3H); ¹³C NMR (CD₃OD) δ 178.29, 72.60, 58.08, 57.65, 44.08, 43.72, 42.05, 41.70, 37.42, 37.36, 36.86, 36.66, 35.84, 32.47, 32.17, 31.36, 29.36, 28.52, 27.81, 25.41, 24.09, 22.10, 18.91, 12.65. Anal. (C₂₄H₄₀O₃) C, H.

ent-Chenodeoxycholic Acid (ent-2). Starting with **20** (246 mg, 0.63 mmol), and using a procedure similar to that used to make **ent-1**, **ent-2** (150 mg, 76%) was obtained as a white solid. The purification of this compound was achieved by column chromatography (silica gel, 50% EtOAc/49% hexanes/1% AcOH to 80% EtOAc/19% MeOH/1% AcOH) followed by recrystallization from 1:1 hexane/EtOAc: mp 138–140 °C (2 lit³⁹ mp 143–145 °C); $[\alpha]_D^{25} = -11.1$ ($c = 0.3$, EtOH) (2 lit³⁹ $[\alpha]_D^{25} = +11.2$ ($c = 0.1$, EtOH)); IR 3417, 1644 cm⁻¹; ¹H NMR (CD₃OD) δ 3.81–3.79 (m, 1H), 3.41–3.36 (m, 1H), 0.96 (d, 3H, $J = 6.6$ Hz), 0.93 (s, 3H), 0.70 (s, 3H); ¹³C NMR (CD₃OD) δ 178.35, 73.01, 69.22, 57.48, 51.69, 43.82, 43.34, 41.20, 40.92, 40.64, 36.92, 36.70, 36.39, 36.04, 34.20, 32.50, 32.12, 31.51, 29.37, 24.77, 23.53, 21.93, 18.94, 12.30. Anal. (C₂₄H₄₀O₄) C, H.

(3 β ,5 α ,8 α ,9 β ,10 α ,13 α ,14 β ,17Z)-Pregn-17(20)-en-3-ol (8). Ethyltriphenyl phosphonium bromide (7.35 g, 19.8 mmol, 6 equiv) was added to a flask and dried under high vacuum for 1 h. After filling with N₂, dry THF (80 mL) was added. KO(*t*-Bu) was prepared by adding potassium (0.77 g, 19.8 mmol, 6 equiv) to *t*-butanol (50 mL). The KO(*t*-Bu) was added to the stirred reaction, and the entire mixture was heated to reflux under N₂ for 30 min during which time the mixture turned bright orange as the ylide formed. Compound **7**²¹ (0.96 g, 3.3 mmol, 1 equiv) was dissolved in dry THF (40 mL) and then added to the refluxing solution, which was then stirred at reflux for 2 h. After cooling to room temperature, the solution was poured into brine (200 mL). The aqueous solution was extracted with 1:1 ether/hexanes (100 mL \times 3), and then the combined organic extracts were washed with brine (100 mL \times 2). The organic layer was then dried over Na₂SO₄ and filtered, and the solvent was removed in vacuo to yield a yellow solid. Column chromatography (silica gel, 10% EtOAc/hexanes to 30% EtOAc/hexanes) of the resulting solid yielded product **8** (0.95 g, 95%) as a white solid. An analytical sample of **8** was obtained by recrystallization from 1:1 acetone/hexanes to give thin white needles: mp 186–187 °C; $[\alpha]_D^{25} = -58.7$ ($c = 0.3$, EtOH); IR 3296, 1688 cm⁻¹; ¹H NMR (CDCl₃) δ 5.10 (qt, 1H, $J = 7.2$, 2.0 Hz), 3.67–3.57 (m, 1H), 1.64 (dt, 3H, $J = 7.2$, 2.0 Hz), 0.92 (s, 3H), 0.85 (s, 3H); ¹³C NMR (CDCl₃) δ 150.37, 113.20, 71.79, 56.24, 44.38, 42.04, 40.48, 37.34, 36.40, 35.33, 35.29, 34.59, 31.45, 30.51, 27.12, 26.27, 24.38, 23.30, 20.95, 16.82, 13.07. Anal. (C₂₁H₃₄O) C, H.

(3 β ,5 α ,8 α ,9 β ,10 α ,13 α ,14 β ,17Z)-Pregn-17(20)-en-3-ol, Acetate (9). Compound **8** (1.33 g, 4.4 mmol, 1 equiv), 4-dimethylaminopyridine (54 mg, 0.44 mmol, 0.1 equiv), acetic anhydride (6.24 mL, 66 mmol, 15 equiv), and pyridine (30 mL) were added to a dry flask and stirred under N₂ for 30 min at room temperature. The reaction mixture was poured into water (200 mL), and a white solid formed. The aqueous solution was then extracted with 1:1 hexanes/EtOAc (200 mL \times 3). The combined organic extracts were then washed with 1 N HCl (200 mL) and brine (200 mL) and dried over Na₂SO₄. The solution was filtered, and the solvent was removed in vacuo to yield a pale green solid. This solid was passed through silica gel, eluting with 10% EtOAc/hexanes to yield product **9** (1.52 g, 100%) as a pale white solid. An analytical sample of **9** was obtained by recrystallization from 1:1 acetone/hexanes to give thin white plates: mp 114–117 °C; $[\alpha]_D^{25} = -75.9$ ($c = 0.4$, EtOH); IR 1738 cm⁻¹; ¹H NMR (CDCl₃) δ 5.10 (qt, 1H, $J = 7.2$, 2.0 Hz), 4.76–4.66 (m, 1H), 2.01 (s, 3H), 1.63 (dt, 3H, $J = 7.2$, 2.0 Hz), 0.93 (s, 3H), 0.84 (s, 3H). ¹³C NMR (CDCl₃) δ 170.58, 150.25, 113.20, 74.27, 56.24, 44.35, 41.82, 40.43, 37.31, 35.26,

34.96, 34.58, 32.16, 31.42, 26.93, 26.56, 25.15, 24.35, 23.24, 21.42, 20.95, 16.80, 13.05. Anal. (C₂₃H₃₆O₂) C, H.

(3 β ,5 α ,8 α ,9 β ,10 α ,13 α ,14 β ,20S,22E)-3-(Acetyloxy)chola-16,22-dien-24-oic Acid, Methyl Ester (10). A flask was dried under high vacuum and then back-filled with N₂. To this flask was added dry toluene (30 mL), diethylaluminumchloride (5.51 mL, 9.92 mmol, 2 equiv, 1.8 M in toluene), and methyl propiolate (0.53 mL, 5.95 mmol, 1.2 equiv). This yellow solution was stirred under N₂ at room temperature for 30 min, after which **9** (1.71 g, 4.96 mmol, 1 equiv) dissolved in dry toluene (20 mL) was added. After the solution was stirred for 24 h, TLC still indicated that some starting material was present. Therefore, a flask was again dried under high vacuum and filled with N₂. Dry toluene (10 mL), diethylaluminumchloride (5.51 mL, 9.92 mmol, 2 equiv, 1.8 M in toluene), and methyl propiolate (0.53 mL, 5.95 mmol, 1.2 equiv) were added, and the yellow solution was stirred for 30 min after which it was added to the reaction. After stirring for another 24 h, the reaction mixture was poured on to saturated aqueous NaHCO₃ (200 mL). A yellow solid precipitated, and this was removed by filtration through a pad of Celite. The aqueous layer was then extracted with Et₂O (150 mL \times 3). The organic extracts were combined, washed with brine (200 mL), and dried over Na₂SO₄. After the solution was filtered, the solvent was removed in vacuo to yield a yellow solid. Column chromatography (silica gel, 5% EtOAc/hexanes to 10% EtOAc/hexanes) of the product gave product **10** (1.90 g, 89%) as a pale white solid. An analytical sample of **10** was recrystallized from a mixture of 1:1 acetone/hexanes to give white needles: mp 106–107 °C; $[\alpha]_D^{25} = -75.9$ ($c = 0.4$, EtOH); IR 1728, 1651, 1615 cm⁻¹; ¹H NMR (CDCl₃) δ 6.92 (dd, 1H, $J = 15.6$, 7.5 Hz), 5.80 (d, 1H, $J = 15.6$ Hz), 5.38 (s, 1H), 4.76–4.67 (m, 1H), 3.72 (s, 3H), 3.02–2.97 (m, 1H), 2.01 (s, 3H), 1.17 (d, 3H, $J = 6.9$ Hz), 0.94 (s, 3H), 0.73 (s, 3H); ¹³C NMR (CDCl₃) δ 170.61, 167.33, 156.96, 153.79, 123.98, 118.65, 74.21, 57.25, 51.41, 47.28, 41.92, 40.97, 35.29, 34.97, 34.94, 34.77, 34.36, 32.22, 31.02, 26.88, 26.52, 26.24, 23.24, 21.43, 20.52, 19.61, 16.38. Anal. (C₂₇H₄₀O₄) C, H.

(3 β ,5 α ,8 α ,9 β ,10 α ,13 α ,14 β ,17 α ,20S)-3-(Acetyloxy)cholan-24-oic Acid, Methyl Ester (11). Palladium on carbon (0.50 g, 5%), **10** (1.75 g, 4.08 mmol), and methanol (150 mL) were added to a hydrogenation bottle. The mixture was hydrogenated for 2 h at 60 psi, after which time the solution was passed through Celite to remove the palladium catalyst. The solvent was removed in vacuo to give a white solid. Column chromatography (silica gel, 5% EtOAc/hexanes to 15% EtOAc/hexanes) of the product to remove minor amounts of other hydrogenation products gave **11** (1.58 g, 90%) as a white solid. An analytical sample of product **11** was obtained by recrystallization from 1:1 acetone/hexanes to give a fluffy white solid: mp 127–129 °C; $[\alpha]_D^{25} = -50.8$ ($c = 0.3$, EtOH); IR 1738 cm⁻¹; ¹H NMR (CDCl₃) δ 4.72–4.65 (m, 1H), 3.63 (s, 3H), 2.00 (s, 3H), 0.90 (s, 3H), 0.88 (d, 3H, $J = 7.5$ Hz), 0.61 (s, 3H). ¹³C NMR (CDCl₃) δ 174.65, 170.53, 74.28, 56.40, 55.89, 51.39, 42.64, 41.79, 40.31, 40.04, 35.68, 35.27, 34.94, 34.48, 32.15, 30.95, 30.90, 28.11, 26.93, 26.53, 26.23, 24.09, 23.25, 21.39, 20.73, 18.18, 11.94. Anal. (C₂₇H₄₄O₄) C, H.

(8 α ,9 β ,10 α ,13 α ,14 β)-Androst-4-ene-3,17-dione (12). *ent*-Steroid **3**^{19, 20} (2.68 g, 9.3 mmol) was dissolved in acetone (100 mL), and while stirring, Jones reagent was added dropwise to this solution until a yellow color persisted. The solution was stirred at room temperature for 30 min, after which time *i*-PrOH was added dropwise to quench any remaining Jones reagent. The reaction mixture was poured into brine (300 mL), and the aqueous solution was extracted with EtOAc (200 mL \times 3). The organic extracts were combined, dried over Na₂SO₄, and filtered. After solvent removal in vacuo, a brown solid remained. This solid was passed through silica gel, eluting with 50% EtOAc/hexanes to yield product **12** (2.33 g, 88%) as a white solid. An analytical sample of product **12** was obtained by recrystallization from 1:1 acetone/hexanes to give a white solid: mp 173–174 °C; $[\alpha]_D^{25} = -180.9$ ($c = 0.4$, EtOH); IR 1736, 1667, 1615 cm⁻¹; ¹H NMR (CDCl₃) δ 5.69 (s, 1H), 1.16 (s, 3H), 0.86 (s, 3H); ¹³C NMR (CDCl₃) δ 220.26, 199.13, 170.23, 123.93, 53.61, 50.62, 47.33, 38.46, 35.58, 35.50, 34.94,

33.74, 32.39, 31.08, 30.55, 21.57, 20.13, 17.20, 13.54. Anal. (C₁₉H₂₆O₂) C, H.

(8 α ,9 β ,10 α ,13 α ,14 β)-Androsta-4,6-diene-3,17-dione (13). In a flask, compound **12** (2.33 g, 8.1 mmol, 1 equiv) was dissolved in glacial AcOH (25 mL) and toluene (10 mL). Tetrachloro-1,4-benzoquinone (*p*-chloranil, 3 g, 12.2 mmol, 1.5 equiv) was added, and the entire mixture was heated at reflux for 1 h, during which time the green solution turned dark orange. After cooling to room temperature, the solution was diluted with EtOAc (250 mL), and this organic solution was washed with water (100 mL), saturated aqueous NaHCO₃ (100 mL), and water (100 mL). The organic layer was dried over Na₂SO₄ and filtered, and the solvent was removed in vacuo to yield a brown solid. Product **13** had the same *R_f* as the starting material on TLC. Column chromatography (silica gel, 10% EtOAc/hexanes to 30% EtOAc/hexanes) of the solid gave product **13** (1.72 g, 75%) as a beige solid. An analytical sample of **13** was obtained by recrystallization from a mixture of 1:1 acetone/EtOAc to give a crystalline beige solid: mp 169–171 °C; [α]_D²⁵ = –121.2 (*c* = 0.3, EtOH); IR 1741, 1662, 1614, 1579 cm⁻¹; ¹H NMR (CDCl₃) δ 6.16 (s, 2H), 5.67 (s, 1H), 1.11 (s, 3H), 0.94 (s, 3H); ¹³C NMR (CDCl₃) δ 219.47, 199.28, 162.87, 138.32, 128.65, 124.04, 50.59, 48.57, 48.18, 36.88, 36.00, 35.52, 33.77, 33.71, 31.13, 21.29, 19.84, 16.22, 13.58. Anal. (C₁₉H₂₄O₂) C, H.

(6 β ,7 β ,8 α ,9 β ,10 α ,13 α ,14 β)-6,7-Epoxyandrosta-4-ene-3,17-dione (14). Compound **13** (1.72 g, 6.05 mmol, 1 equiv) was dissolved in CH₂Cl₂ (50 mL) and chilled in an ice/water bath. *m*-Chloroperoxybenzoic acid (~70% purity, 2.61 g, 15.13 mmol, 2.5 equiv) was added, and the solution was stirred at 4 °C for 2 days. 15% aqueous Na₂S₂O₃ (50 mL) was added to the reaction, and it was stirred for 30 min at room temperature. The organic layer was separated and washed with 15% aqueous Na₂CO₃ (100 mL). The combined aqueous layers were then extracted with CH₂Cl₂ (100 mL). The organic layers were combined, dried over Na₂SO₄, and filtered, and the solvent was removed in vacuo to give a yellow oil. Column chromatography (silica gel, 10% EtOAc/hexanes to 30% EtOAc/hexanes) of this oil gave product **14** (1.06 g, 58%) as a white solid and recovered starting material **13** (0.23 g, 14%) as a white solid. An analytical sample of **14** was obtained by recrystallization from a mixture of 1:1 acetone/hexanes to give a white solid: mp 214–216 °C; [α]_D²⁵ = –116.1 (*c* = 0.3, EtOH); IR 1737, 1676, 1621 cm⁻¹; ¹H NMR (CDCl₃) δ 6.12 (s, 1H), 3.51 (d, *J* = 3.6 Hz), 3.45 (d, *J* = 3.3 Hz), 1.10 (s, 3H), 0.93 (s, 3H); ¹³C NMR (CDCl₃) δ 219.06, 197.84, 161.64, 131.43, 53.46, 52.55, 47.78, 46.83, 41.00, 35.64, 35.59, 34.35, 33.97, 33.86, 31.08, 21.40, 19.25, 17.23, 13.57. Anal. (C₁₉H₂₄O₃) C, H.

(5 α ,7 β ,8 α ,9 β ,10 α ,13 α ,14 β)-7-Hydroxyandrosta-3,17-dione (15). Pyridine was dried over CaH₂ and freshly distilled before each experiment. Compound **14** (192 mg, 0.64 mmol) was dissolved in dry pyridine (10 mL) in a hydrogenation bottle. Palladium on carbon (5%, 64 mg) was added, and the solution was hydrogenated overnight for 18 h at 30 psi. It was then filtered through a pad of Celite, eluting with MeOH. After removal of the solvent in vacuo, a brown solid remained. This solid was dissolved in CH₂Cl₂, and the solution was washed with 1 N HCl (100 mL \times 2). After drying over Na₂SO₄ and filtering, the solvent was removed in vacuo to yield a product that was purified by column chromatography (silica gel, 40% EtOAc/hexanes to 70% EtOAc/hexanes) to give product **15** (125 mg, 64%) as a white solid. An analytical sample of **15** was obtained by recrystallization from 1:1 acetone/hexane as white crystals: mp 235–236 °C; [α]_D²⁵ = –84.5 (*c* = 0.3, EtOH); IR 3447, 1737, 1692 cm⁻¹; ¹H NMR (CDCl₃) δ 4.06–4.05 (m, 1H), 3.39 (t, 1H, *J* = 14.4 Hz), 1.01 (s, 3H), 0.87 (s, 3H); ¹³C NMR (CDCl₃) δ 221.02, 213.08, 67.03, 47.48, 45.57, 45.50, 43.06, 38.83, 36.81, 36.67, 35.77, 35.38, 34.15, 33.59, 31.21, 21.76, 21.32, 20.25, 13.39. Anal. (C₁₉H₂₈O₃) C, H.

(3 β ,5 α ,7 β ,8 α ,9 β ,10 α ,13 α ,14 β)-3,7-Dihydroxyandrostan-17-one (16). To a dry flask was added **15** (354 mg, 1.16 mmol, 1 equiv) dissolved in dry THF (50 mL). While under N₂, the solution was cooled to –42 °C in a bath of acetonitrile and dry ice. Lithium tri-*t*-butoxyaluminumhydride (1.45 mL, 1.45 mmol, 1.25 equiv, 1 M

in THF) was added dropwise, and the solution was stirred for 2 h at –42 °C under N₂. After seeing that the reaction was not complete, additional lithium tri-*t*-butoxyaluminumhydride was added until minimal starting material was present. The reaction was carefully quenched with 3 N HCl and then warmed to room temperature. EtOAc (250 mL) was added, and the organic solution was washed with saturated aqueous NaHCO₃ (150 mL) and brine (150 mL). The organic layer was dried over Na₂SO₄ and filtered, and the solvent was removed in vacuo to give a white solid. Column chromatography (silica gel, 20% EtOAc/hexanes to 50% EtOAc/hexanes) yielded product **16** (313.5 mg, 88%) as a clear oil along with recovered starting material **15** (25 mg, 7%): oil **16** had [α]_D²⁵ = –59.4 (*c* = 0.4, EtOH); IR 3413, 1737 cm⁻¹; ¹H NMR (CDCl₃) δ 3.93–3.92 (m, 1H), 3.43–3.35 (m, 1H), 0.87 (s, 3H), 0.80 (s, 3H); ¹³C NMR (CDCl₃) δ 221.46, 71.58, 67.09, 47.40, 45.61, 41.36, 39.63, 38.89, 35.79, 35.26, 35.11, 34.77, 33.07, 31.31, 30.55, 22.58, 21.28, 19.78, 13.28; Anal. (C₁₉H₃₀O₃) C, H.

(3 β ,5 α ,7 β ,8 α ,9 β ,10 α ,13 α ,14 β ,17Z)-Pregn-17(20)-ene-3,7-diol (17). Starting with **16** (314 mg, 1.02 mmol), a procedure similar to that used to make **8** was used to obtain product **17** (313 mg, 96%) as a white solid. An analytical sample of **17** was obtained by recrystallization from 1:1 acetone/hexanes to give a white solid: mp 168–169 °C; [α]_D²⁵ = –15.2 (*c* = 0.3, CHCl₃); IR 3295, 3214, 1633 cm⁻¹; ¹H NMR (CDCl₃) δ 5.13 (qt, 1H, *J* = 6.9, 2.1 Hz), 3.91–3.90 (m, 1H), 3.51–3.41 (m, 1H), 0.91 (s, 3H), 0.87 (s, 3H); ¹³C NMR (CDCl₃) δ 149.71, 113.54, 71.98, 68.44, 50.38, 44.26, 41.45, 39.86, 38.99, 36.85, 35.27, 35.09, 34.53, 32.83, 31.43, 30.64, 24.03, 22.71, 20.73, 16.51, 13.10. Anal. (C₂₁H₃₄O₂) C, H.

(3 β ,5 α ,7 β ,8 α ,9 β ,10 α ,13 α ,14 β ,17Z)-Pregn-17(20)-ene-3,7-diol, Diacetate (18). Starting with **17** (237 mg, 0.74 mmol, 1 equiv), a procedure similar to that used to make **9** was followed. Several changes made included doubling the equiv of 4-dimethylaminopyridine (18 mg, 0.15 mmol, 0.2 equiv) and acetic anhydride (2.10 mL, 22 mmol, 30 equiv) and running the reaction overnight (~16 h). This gave product **18** (288 mg, 97%) as a white solid. An analytical sample of **18** was obtained by recrystallization from methanol to give fine white needles: mp 91–93 °C; [α]_D²⁵ = –39.4 (*c* = 0.4, CHCl₃); IR 1736, 1655 cm⁻¹; ¹H NMR (CDCl₃) δ 5.15–5.08 (qt, 1H, *J* = 6.9, 2.0 Hz), 4.94–4.91 (m, 1H), 4.63–4.53 (m, 1H), 2.02 (s, 6H), 0.93 (s, 3H), 0.85 (s, 3H); ¹³C NMR (CDCl₃) δ 170.61, 170.38, 149.60, 113.57, 74.09, 71.07, 50.27, 44.28, 40.91, 37.47, 36.76, 34.82 (C \times 2), 34.59, 34.06, 31.27 (C \times 2), 26.74, 23.83, 22.60, 21.49, 21.45, 20.76, 16.41, 13.05; Anal. (C₂₅H₃₈O₄) C, H.

(3 β ,5 α ,7 β ,8 α ,9 β ,10 α ,13 α ,14 β ,20S,22E)-3,7-Bis(acetyloxy)cholan-16,22-dien-24-oic Acid, Methyl Ester (19). Starting with **18** (426 mg, 1.06 mmol), a procedure similar to that used to prepare **10** was utilized to obtain product **19** (241 mg, 47%) as a pale yellow oil and recovered starting material **18** (198 mg, 46%). Oil **19** had [α]_D²⁵ = –23.9 (*c* = 0.6, CHCl₃); IR 1731, 1650, 1617 cm⁻¹; ¹H NMR (CDCl₃) δ 6.91 (dd, 1H, *J* = 15.5, 8.0 Hz), 5.80 (dd, 1H, *J* = 15.6, 0.9 Hz), 5.36 (s, 1H), 4.94–4.95 (m, 1H), 4.63–4.53 (m, 1H), 3.71 (s, 3H), 3.00 (t, 1H, *J* = 7.1 Hz), 2.04 (s, 3H), 2.01 (s, 3H), 1.17 (d, 3H, *J* = 6.9 Hz), 0.94 (s, 3H), 0.74 (s, 3H); ¹³C NMR (CDCl₃) δ 170.59, 170.38, 167.27, 156.54, 153.53, 123.98, 118.80, 74.01, 71.40, 51.52, 51.44, 47.37, 41.00, 36.50, 35.32, 34.96, 34.79, 34.59, 34.47, 34.36, 31.25, 30.54, 26.68, 22.55, 21.57, 21.43, 20.34, 19.53, 16.09.

(3 β ,5 α ,7 β ,8 α ,9 β ,10 α ,13 α ,14 β ,17 α ,20S)-3,7-Bis(acetyloxy)cholan-24-oic Acid, Methyl Ester (20). Starting with compound **19** (256 mg, 0.53 mmol, 1 equiv), the procedure used to make product **11** was utilized to obtain **20** (246 mg, 95%) as a white solid. An analytical sample of product **20** was obtained by recrystallization from 1:1 methanol/hexanes to give a white solid: mp 122–124 °C; [α]_D²⁵ = –18.4 (*c* = 0.5, CHCl₃); IR 1734 cm⁻¹; ¹H NMR (CDCl₃) δ 4.87–4.86 (m, 1H), 4.63–4.52 (m, 1H), 3.65 (s, 1H), 2.04 (s, 3H), 2.02 (s, 3H), 0.92 (s, 3H), 0.91 (d, 3H, *J* = 6.0 Hz), 0.63 (s, 3H); ¹³C NMR (CDCl₃) δ 174.65, 170.59, 170.38, 74.12, 71.19, 55.70, 51.45, 50.35, 42.64, 40.91, 39.43, 37.84, 35.23, 34.85, 34.74, 34.58, 34.01, 31.27, 30.93, 30.90, 27.97, 26.74, 23.50, 22.63, 21.55, 21.45, 20.60, 18.23, 11.64; Anal. (C₂₉H₄₆O₆) C, H.

cmc Determination. These experiments were performed in a similar manner as previously described.²⁸ Briefly, sodium salts of each bile acid were made by dissolving the bile acid in MeOH, followed by the addition of an appropriate amount of NaOH to neutralize the solution. After concentrating the solution, the bile salts were precipitated by the addition of Et₂O, and then the white solids were collected by filtration. Stock solutions were prepared by weighing each bile acid sodium salt on a Thermo Electron Corporation Orion-Cahn C-33 microbalance, and appropriate concentrations were made by diluting this stock solution. A separate stock solution was made for each individual experiment.

Aqueous solutions (2 mL) were made for each **1** and *ent-1* concentration tested. However, due to a limited amount of *ent-2*, 200 μ L aqueous solutions of **2** and *ent-2* were made for each concentration. The aqueous bile acid solutions were rotated with excess crystalline Orange OT (TCI America) for 3 days at room temperature. The solution was filtered through a 0.22 μ m filter unit (25 mm Fisherbrand for **1** and *ent-1* and 13 mm Millipore for **2** and *ent-2*) to remove excess crystalline dye. Absorbance readings were taken on each sample at 483 nm using a Beckman Coulter DU 7400 UV-vis spectrophotometer, and these values were plotted as a function of concentration.

A best-fit linear line (Microsoft Excel) was drawn through the first group of points that showed little increase in absorbance (4 points for **1** and *ent-1* and 9–10 points for **2** and *ent-2*). Another best-fit linear line was drawn through the points where absorbance increased markedly in a linear fashion (9 points for **1** and *ent-1*, and 3–4 points for **2** and *ent-2*). The intersection of these two lines was taken as the cmc. The cmc determinations were performed in triplicate for each bile acid, and the reported cmc was taken as the average of these three experiments. *P*-Values were calculated using an unpaired two-tailed Student's *t*-test (Microsoft Excel).

Transient Transfection Assays. HEK293 cells were maintained at 37 °C, 5% CO₂ in DMEM containing 10% super-stripped FBS. Cells were plated at 4.0 \times 10⁴ cells per well in 96-well plates and transfected with calcium phosphate as described previously² using the UAS luciferase reporter (50 ng) in combination with GAL4-ligand binding domain fusion proteins of hFXR (15 ng), GAL4-hVDR (15 ng), or GAL4-hPXR (15 ng), β -galactosidase (10 ng), and pGEM to a total of 150 ng/well. Ligands were added 6–8 h later in delipidated media. Cells were harvested 14–16 h later and assayed for luciferase and β -galactosidase activity. Luciferase values were normalized for transfection efficiency using β -galactosidase and expressed as RLU of triplicate assays. For antagonist experiments, 1 μ M GW4064 was added in combination with increasing concentrations of bile acid in the presence of GAL4-hFXR and normalized against vehicle control at each concentration. Full-length hFXR (15 ng) was tested in combination with hRXR α (15 ng) for activation by *ent*-bile acids using a reporter consisting of three copies of the mouse IBABP IR-1 response element upstream of TK-luc (FXREx3-TK-luc).²

Cell Culture Treatment. Huh7 cells were seeded at 2 \times 10⁵ cells/well in 12-well plates using DMEM (high glucose, 4.5 g/L glucose) with 10% FBS, 100 U/mL penicillin, and 100 μ g/mL streptomycin and maintained at 37 °C and 5% CO₂. The next day, ligands were added in DMEM (low glucose, 1 g/L glucose) containing 5% charcoal-stripped FBS, 100 U/mL penicillin, and 100 μ g/mL streptomycin, and cells were harvested for RNA after 18 h. HepG2 (human hepatoma) cells were maintained according to Yu et al.⁴⁰ Briefly, cells were maintained at 37 °C and 5% CO₂ in DMEM containing 10% FBS, 100 U/mL penicillin, 100 μ g/mL streptomycin, 1 mM sodium pyruvate, and 5 mM HEPES. For treatment with *ent*-bile acids, cells were seeded at 3 \times 10⁵ cells/well in 6-well plates in M199 medium containing 10% FBS, 100 U/mL penicillin, 100 μ g/mL streptomycin, and 25 mM HEPES. After 24 h, the media was substituted with media containing ligands and incubated for 18 h before harvesting RNA as described next. Caco-2 cells were cultured in high glucose DMEM supplemented with 15% heat-inactivated FBS. Cells were plated in 6-well plates, and media were changed every 3 days. Twenty-three days after

reaching confluency, cells were treated with ligands in high glucose DMEM supplemented with 15% charcoal-stripped, heat-inactivated FBS. After 6 days of treatment, cells were harvested for RNA as described next.

RNA Isolation and Real-Time PCR. Total RNA was isolated using RNASat60 (Tel-Test) and processed for real-time PCR on an ABI Prism 7900 HT system (ABI Advanced Technologies Inc.) as described.⁴¹ Each reaction contained 12.5 ng of cDNA, 150 nM forward and reverse primers, and 2X SYBR green buffer (Invitrogen). QPCR primers are shown in the Supporting Information (Table 3). Gene expression analysis was performed using the $\Delta\Delta$ Ct method normalizing against cyclophilin, and the fold activation was calculated relative to vehicle treated cells.

Determination of Intracellular cAMP Levels. HEK293 cells were seeded in 24-well plates (0.5 \times 10⁶ cells/well) at 37 °C and incubated for 24 h. The cells were then transfected with TGR5 expression vector or control empty vector. After 2 days, the cells were treated with or without the test compound for 30 min at 37 °C in fresh medium containing 0.2 mM 3-isobutyl-1-methylxanthine (IBMX). After cell lysis, intracellular cAMP levels were determined using a cAMP kit (GE healthcare). The TGR5 synthetic agonist benzyl 2-keto-6-methyl-4-(2-thienyl)-1,2,3,4-tetrahydropyrimidine-5-carboxylate (**21**) was obtained as a gift from Dr. Johan Auwerx (IGBMC).¹⁸

Data Analysis for Receptor Biology. For comparison between two groups, the unpaired Student's *t*-test was performed. One-way ANOVA followed by Dunnett's test was used for multiple comparisons against a vehicle control group. All tests were performed using the software program Primer of Biostatistics (McGraw Hill).

Acknowledgment. This work was supported by NIH Grants GM47969 (D.F.C.), 5-T32-HL07275 (B.W.K.), U19-DK62434 (D.J.M.), the Howard Hughes Medical Institute (HHMI, D.J.M.), and the Robert A. Welch Foundation (D.J.M.). D.J.M. is an Investigator, and C.L.C. is an Associate of HHMI.

Supporting Information Available: List of carbon and hydrogen elemental analyses for *ent-1*, *ent-2*, **8–18**, and **20** (Table 2), as well as a list of the human primers used for QPCR (Table 3). This material is available free of charge via the Internet at <http://pubs.acs.org>.

References

- (1) Pellicciari, R.; Costantino, G.; Fiorucci, S. Farnesoid X receptor: From structure to potential clinical applications. *J. Med. Chem.* **2005**, *48*, 5383–5403.
- (2) Makishima, M.; Okamoto, A. Y.; Repa, J. J.; Tu, H.; Learned, R. M.; Luk, A.; Hull, M. V.; Lustig, K. D.; Mangelsdorf, D. J.; Shan, B. Identification of a nuclear receptor for bile acids. *Science (Washington, DC, U.S.)* **1999**, *284*, 1362–1365.
- (3) Parks, D. J.; Blanchard, S. G.; Bledsoe, R. K.; Chandra, G.; Consler, T. G.; Kliewer, S. A.; Stimmel, J. B.; Willson, T. M.; Zavacki, A. M.; Moore, D. D.; Lehmann, J. M. Bile acids: Natural ligands for an orphan nuclear receptor. *Science (Washington, DC, U.S.)* **1999**, *284*, 1365–1368.
- (4) Wang, H. B.; Chen, J.; Hollister, K.; Sowers, L. C.; Forman, B. M. Endogenous bile acids are ligands for the nuclear receptor FXR BAR. *Mol. Cell* **1999**, *3*, 543–553.
- (5) Makishima, M. Nuclear receptors as targets for drug development: Regulation of cholesterol and bile acid metabolism by nuclear receptors. *J. Pharmacol. Sci.* **2005**, *97*, 177–183.
- (6) Staudinger, J. L.; Goodwin, B.; Jones, S. A.; Hawkins-Brown, D.; MacKenzie, K. I.; Latour, A.; Liu, Y. P.; Klaassen, C. D.; Brown, K. K.; Reinhard, J.; Willson, T. N.; Koller, B. H.; Kliewer, S. A. The nuclear receptor PXR is a lithocholic acid sensor that protects against liver toxicity. *Proc. Natl. Acad. Sci. U.S.A.* **2001**, *98*, 3369–3374.
- (7) Xie, W.; Radominska-Pandya, A.; Shi, Y. H.; Simon, C. M.; Nelson, M. C.; Ong, E. S.; Waxman, D. J.; Evans, R. M. An essential role for nuclear receptors SXR/PXR in detoxification of cholestatic bile acids. *Proc. Natl. Acad. Sci. U.S.A.* **2001**, *98*, 3375–3380.
- (8) Makishima, M.; Lu, T. T.; Xie, W.; Whitfield, G. K.; Domoto, H.; Evans, R. M.; Haussler, M. R.; Mangelsdorf, D. J. Vitamin D receptor as an intestinal bile acid sensor. *Science (Washington, DC, U.S.)* **2002**, *296*, 1313–1316.

- (9) Kliewer, S. A.; Willson, T. M. Regulation of xenobiotic and bile acid metabolism by the nuclear pregnane X receptor. *J. Lipid Res.* **2002**, *43*, 359–64.
- (10) Liu, Y. P.; Binz, J.; Numerick, M. J.; Dennis, S.; Luo, G. Z.; Desai, B.; MacKenzie, K. I.; Mansfield, T. A.; Kliewer, S. A.; Goodwin, B.; Jones, S. A. Hepatoprotection by the farnesoid X receptor agonist GW4064 in rat models of intra- and extrahepatic cholestasis. *J. Clin. Invest.* **2003**, *112*, 1678–1687.
- (11) Szapary, P. O.; Wolfe, M. L.; Bloedon, L. T.; Cucchiara, A. J.; DerMarderosian, A. H.; Cirigliano, M. D. Guggulipid for the treatment of hypercholesterolemia—A randomized controlled trial. *J. Am. Med. Assoc.* **2003**, *290*, 765–772.
- (12) Owsley, E.; Chiang, J. Y. Guggulsterone antagonizes farnesoid X receptor induction of bile salt export pump but activates pregnane X receptor to inhibit cholesterol 7 α -hydroxylase gene. *Biochem. Biophys. Res. Commun.* **2003**, *304*, 191–195.
- (13) Zollner, G.; Marschall, H. U.; Wagner, M.; Trauner, M. Role of nuclear receptors in the adaptive response to bile acids and cholestasis: Pathogenetic and therapeutic considerations. *Mol. Pharmacol.* **2006**, *3*, 231–251.
- (14) Yee, Y. K.; Chintalacheruvu, S. R.; Lu, J.; Nagpal, S. Vitamin D receptor modulators for inflammation and cancer. *Mini Rev. Med. Chem.* **2005**, *5*, 761–778.
- (15) Gombart, A. F.; Luong, Q. T.; Koeffler, H. P. Vitamin D compounds: Activity against microbes and cancer. *Anticancer Res.* **2006**, *26*, 2531–2542.
- (16) Kawamata, Y.; Fujii, R.; Hosoya, M.; Harada, M.; Yoshida, H.; Miwa, M.; Fukusumi, S.; Habata, Y.; Itoh, T.; Shintani, Y.; Hinuma, S.; Fujisawa, Y.; Fujino, M. A G protein-coupled receptor responsive to bile acids. *J. Biol. Chem.* **2003**, *278*, 9435–9440.
- (17) Maruyama, T.; Miyamoto, Y.; Nakamura, T.; Tamai, Y.; Okada, H.; Sugiyama, E.; Nakamura, T.; Itadani, H.; Tanaka, K. Identification of membrane-type receptor for bile acids (M-BAR). *Biochem. Biophys. Res. Commun.* **2002**, *298*, 714–719.
- (18) Watanabe, M.; Houten, S. M.; Matak, C.; Christoffolete, M. A.; Kim, B. W.; Sato, H.; Messaddeq, N.; Harney, J. W.; Ezaki, O.; Kodama, T.; Schoonjans, K.; Bianco, A. C.; Auwerx, J. Bile acids induce energy expenditure by promoting intracellular thyroid hormone activation. *Nature (London, U.K.)* **2006**, *439*, 484–489.
- (19) Michéli, R. A.; Hajos, Z. G.; Cohen, N.; Parrish, D. R.; Portland, L. A.; Sciamanna, W.; Scott, M. A.; Wehrli, P. A. Total syntheses of optically active 19-norsteroids. (+)-Estr-4-ene-3,17-dione and (+)-13 β -ethylgon-4-ene-3,17-dione. *J. Org. Chem.* **1975**, *40*, 675–681.
- (20) Rychnovsky, S. D.; Mickus, D. E. Synthesis of *ent*-cholesterol, the unnatural enantiomer. *J. Org. Chem.* **1992**, *57*, 2732–2736.
- (21) Katona, B. W.; Krishnan, K.; Cai, Z. Y.; Manion, B. D.; Benz, A.; Taylor, A.; Evers, A. S.; Zorumski, C. F.; Mennerick, S.; Covey, D. F. Neurosteroid analogues. 12. Potent enhancement of GABA-mediated chloride currents at GABAA receptors by *ent*-androgens. *Eur. J. Med. Chem.*, in press.
- (22) Han, M. C.; Zorumski, C. F.; Covey, D. F. Neurosteroid analogues. 4. The effect of methyl substitution at the C-5 and C-10 positions of neurosteroids on electrophysiological activity at GABA(A) receptors. *J. Med. Chem.* **1996**, *39*, 4218–4232.
- (23) Templeton, J. F.; Kumar, V. P. S. Synthesis of ring-A and -B substituted 17 α -acetoxypregnan-20-one derivatives with potential activity on the digitalis receptor in cardiac muscle. *J. Chem. Soc., Perkin Trans. 1* **1987**, 1361–1368.
- (24) Westover, E. J.; Covey, D. F. First synthesis of *ent*-desmosterol and its conversion to *ent*-deuterocholesterol. *Steroids* **2003**, *68*, 159–166.
- (25) Tochtrop, G. P.; DeKoster, G. T.; Cistola, D. P.; Covey, D. F. Synthesis of [3,4-C-13(2)]-enriched bile salts as NMR probes of protein–ligand interactions. *J. Org. Chem.* **2002**, *67*, 6764–6771.
- (26) Lai, C. K.; Byon, C. Y.; Gut, M. Synthesis of 3 α ,7 α -dihydroxy-5 β -androstan-17-one. *Steroids* **1983**, *42*, 707–711.
- (27) Wovkulich, P. M.; Batcho, A. D.; Uskoković, M. R. Stereoselective introduction of steroid side chains. Synthesis of chenodeoxycholic acid. *Helv. Chim. Acta* **1984**, *67*, 612–615.
- (28) Roda, A.; Hofmann, A. F.; Mysels, K. J. The influence of bile salt structure on self-association in aqueous solutions. *J. Biol. Chem.* **1983**, *258*, 6362–6370.
- (29) Nair, P. P.; Kritchevsky, D. *The Bile Acids: Chemistry, Physiology, and Metabolism*; Plenum Press: New York, 1971; Vol. 1.
- (30) Carnahan, V. E.; Redinbo, M. R. Structure and function of the human nuclear xenobiotic receptor PXR. *Curr. Drug Metab.* **2005**, *6*, 357–367.
- (31) Yu, J.; Lo, J. L.; Huang, L.; Zhao, A.; Metzger, E.; Adams, A.; Meinke, P. T.; Wright, S. D.; Cui, J. Lithocholic acid decreases expression of bile salt export pump through farnesoid X receptor antagonist activity. *J. Biol. Chem.* **2002**, *277*, 31441–31447.
- (32) Maloney, P. R.; Parks, D. J.; Haffner, C. D.; Fivush, A. M.; Chandra, G.; Plunket, K. D.; Creech, K. L.; Moore, L. B.; Wilson, J. G.; Lewis, M. C.; Jones, S. A.; Willson, T. M. Identification of a chemical tool for the orphan nuclear receptor FXR. *J. Med. Chem.* **2000**, *43*, 2971–2974.
- (33) Mi, L. Z.; Devarakonda, S.; Harp, J. M.; Han, Q.; Pellicciari, R.; Willson, T. M.; Khorasanizadeh, S.; Rastinejad, F. Structural basis for bile acid binding and activation of the nuclear receptor FXR. *Mol. Cell* **2003**, *11*, 1093–1100.
- (34) Houten, S. M.; Watanabe, M.; Auwerx, J. Endocrine functions of bile acids. *EMBO J.* **2006**, *25*, 1419–1425.
- (35) Biellmann, J. F. Enantiomeric steroids: Synthesis, physical, and biological properties. *Chem. Rev.* **2003**, *103*, 2019–2033.
- (36) Westover, E. J.; Covey, D. F.; Brockman, H. L.; Brown, R. E.; Pike, L. J. Cholesterol depletion results in site-specific increases in epidermal growth factor receptor phosphorylation due to membrane level effects—Studies with cholesterol enantiomers. *J. Biol. Chem.* **2003**, *278*, 51125–51133.
- (37) Alakoskela, J. M.; Covey, D. F.; Kinnunen, P. K. J. Lack of enantiomeric specificity in the effects of anesthetic steroids on lipid bilayers. *Biochim. Biophys. Acta* **2007**, *1768*, 131–145.
- (38) O’Neil, M. J. *The Merck Index*, 14th ed.; Merck Research Laboratories: Whitehouse Station, NJ, 2006.
- (39) Kametani, T. Studies on the syntheses of heterocyclic and natural compounds. 950. Asymmetric total synthesis of (+)-chenodeoxycholic acid. Stereoselectivity of intramolecular cycloaddition of olefinic *o*-quinodimethanes. *J. Org. Chem.* **1982**, *47*, 2331–2342.
- (40) Yu, J. H.; Lo, J. L.; Huang, L.; Zhao, A.; Metzger, E.; Adam, A.; Meinke, P. T.; Wright, S. D.; Cui, J. S. Lithocholic acid decreases expression of bile salt export pump through farnesoid X receptor antagonist activity. *J. Biol. Chem.* **2002**, *277*, 31441–31447.
- (41) Bookout, A. L.; Cummins, C. L.; Mangelsdorf, D. J. High-throughput real-time quantitative reverse transcription PCR. *Curr. Protocols Mol. Biol.* **2005**, 15.8.1–15.8.21.

JM0707931